

Nonlinear Connections Between Realized Volatility and High/Low Range Information

Blake LeBaron ^{*}

Xia Meng [†]

August 2012

Abstract

In this paper we look at the relationship between daily realized volatility estimates using intraday data and range based estimates using daily high/low price range information. Several classical range based volatility estimators are compared with nonlinear functional forms in mapping range based information onto realized volatility measures. We find that the older range based estimators can be improved by using more generalized nonlinear functions of the high/low range information. We show that these nonlinearities form an important piece of information for understanding the dynamics of prices at high frequencies. We also show that these improved volatility estimates can be used in forecasting future variances and risk measures, and improve on the typical range estimators.

Keywords: Realized volatility, range based volatility, neural networks, nonlinear models, volatility forecasting

^{*}International Business School, Brandeis University, 415 South Street, Mailstop 32, Waltham, MA 02453 - 2728, blebaron@brandeis.edu, www.brandeis.edu/~blebaron. The author is also a research associate at the National Bureau of Economic Research.

[†]Senior Consultant at Bates White Consulting.

1 Introduction

Our empirical understanding and estimation of volatility and risk has been making great progress over the last decade. The use of high frequency data in the estimation and forecasting of volatility has been critical in this process. Volatility estimates built from intraday data produce conditional variance estimates which are orders of magnitude better than what has been previously used.¹ Our work will extend some of these results by connecting the high frequency volatility values to range based estimates using nonparametric and nonlinear techniques. Our goals are to develop a deeper understanding of the latent volatility process itself, and to provide some improved volatility measures which can be used when high frequency pricing series are not available.

In our analysis we utilize the Oxford-Mann Institute’s volatility libraries, (Heber, Lunde, Shephard & Sheppard 2009). These are realized volatility estimates that the authors have built using high frequency data feeds, and provide on their website to researchers. These benchmark series form a core of our work in that we will view these estimates as high precision volatility measures. We will then use contemporaneous range information to explore the connections between daily ranges, and the high frequency measures. We take some of the classic range volatility estimators as our benchmark comparisons.²

Our research on this topic is inspired by a paper coming from a slightly different area, Hutchinson, Lo & Poggio (1994). These authors explore the gains of nonparametric modeling in option pricing. They use various nonlinear nonparametric methods to estimate option pricing relations. Their intention is to race the nonparametric methods with an important parametric comparison, the Black/Scholes model. This can both show the practical power of using a nonparametric approach, and demonstrate how and why the parametric model fails, leading to better understanding of its limitations and assumptions.

Our goals are similar. We will fit high frequency realized volatility estimates to range based volatility estimates, and race these against some of the simple parametric models that are available. We show that for most of our series, we can significantly improve on these models. We use our nonlinear approaches both in the cross section and in the time series risk forecasting context. There we race our improved models against forecasts build from the actual realized volatility series. We show that performance of our modified range estimator is surprisingly close to the realized volatility forecasts. Therefore, it looks like these estimates may prove useful in contexts where only range information is available.

¹ Three recent surveys of this large literature are Andersen, Bollerslev, Christoffersen & Diebold (forthcoming 2012) and Barndorff-Nielsen & Shephard (2010), and McAleer & Medeiros (2008). The basic concept of using high frequency observations to estimate lower frequency volatility goes back to Merton (1980) and French, Schwert & Stambaugh (1987).

²The two basic range based estimators we use follow Parkinson (1980) and Garman & Klass (1980).

In demonstrating that the classic range estimators can be beaten, we open the question of why they do so poorly. They are all built from assumptions which are violated in financial data. The first is that high frequency pricing information does not follow a perfect Brownian motion. Various market frictions enter through market microstructure, and the institutions of trading itself. Research on this in volatility estimation has been very active, and the realized volatility estimator we use has been designed to take this into account.³ The high/low range information we use is not adjusted for market microstructure issues, and it is still not clear how to do this. The second issue in high frequency data is that prices may contain discrete jumps in addition to the continuous Brownian motion.⁴ It is possible these jumps interfere with both our volatility measures, and cause the patterns that we observe in our series. We will perform some simple monte-carlo experiments to show that basic jump models probably are not the cause for what we are seeing. We feel a richer dynamic must be at work.

The next section reviews some of the literature on volatility estimators, and provides a brief description of the estimators that we will be using. In section 3 we will estimate our cross sectional volatility models. We fit daily realized volatility to various functional forms using contemporaneous and lagged range information, and some other pricing information. The models are compared in terms of cross sectional fits, and formal nonlinear specification tests. Section 4 uses the range based volatility estimates in a time series context. We follow much of the risk forecasting literature by building time series from logged volatility estimates.⁵ Our objective is to see how the volatility models compare in a one step ahead variance forecasting context. We simulate the model forecasts out of sample, assuming the econometrician is operating without any of the high frequency information. This provides an estimate of how well these models might perform in a situation where high frequency information is unavailable or unreliable. The final section concludes and provides some information for the future.

2 Daily volatility estimators

High frequency financial data allows for detailed estimates of market volatility. The basic logic is that using higher and higher frequency pricing information will give more detailed volatility estimates. In the case of a continuous time Brownian motion with no market

³ Among papers addressing this problem are Bandi & Russell (2008), Hansen & Lunde (2006), Zhang, Mykland & Ait-Sahalia (2005). We follow Barndorff-Nielsen, Hansen, Lunde & Shephard (2008) and Barndorff-Nielsen, Hansen, Lunde & Shephard (2009) utilizing their realized kernel methods.

⁴ Various papers have addressed the problem of jumps. These include Andersen, Bollerslev & Diebold (2007), Barndorff-Nielsen & Shephard (2004), Corsi, Pirino & Reno (2008) and Fissel & Sun (2010).

⁵We use a multi horizon model developed in Corsi (2009) for this.

frictions there would be little argument about what to do. Use of a simple highest possible frequency estimate of the daily variance would be optimal. Unfortunately, financial markets deviate from this idealized world, and realized volatility can be measured in several ways.

Market frictions and market microstructure noise degrade the performance of ultra high frequency estimators and have led to a large debate about the optimal frequency for sampling prices. This also has led to more sophisticated estimators that use multiple sampling frequencies and nonparametric kernel estimators. A second problem is that price series may contain jumps. The use of Bipower estimators as in Andersen et al. (2007) and Barndorff-Nielsen & Shephard (2004) can give a possible “jump free” estimate of integrated volatility over a day.

This paper will concentrate on the kernel based volatility estimate provided in the Oxford-Man realized volatility (Heber et al. 2009), version 0.2. This data set provides detailed estimates of realized volatility for several different financial returns series, using three types of realized volatility estimators.⁶

The constructed volatility series are built using a weighted sum of a range of covariates over the intraday returns series given in x_j .

$$K(X) = \sum_{h=-H}^H k\left(\frac{h}{H+1}\right) \gamma_h \quad (1)$$

$$\gamma_h = \sum_{j=|h|+1}^n x_j x_{j-|h|} \quad (2)$$

The weighting uses the Parzen kernel function given by,

$$k(x) = \begin{cases} 1 - 6x^2 + 6x^3 & 0 \leq x \leq 1/2 \\ 2(1 - x)^3 & 1/2 \leq x \leq 1 \\ 0 & x > 1 \end{cases} \quad (3)$$

The value $K(X)$ is estimated daily using high frequency returns, x_τ over each day, t . We will refer to this as the realized volatility on day t , or RV_t . Barndorff-Nielsen et al. (2008) recommend this kernel since it has several appealing features including guaranteed nonnegative weights, and $k'(0) = k'(1) = 0$.

Our objective is to link this to several volatility measures using only range based infor-

⁶ Also, see Barndorff-Nielsen et al. (2008) for details. Barndorff-Nielsen et al. (2009) also give details on critical data cleaning procedures that are used before volatilities are estimated.

mation.⁷ The first was developed by Parkinson (1980), and is relatively simple.

$$V_{t,p} = \frac{(\log(H_t) - \log(L_t))^2}{4\log(2)}, \quad (4)$$

where $V_{t,p}$ is the estimate of daily volatility, and H_t and L_t are the daily high and low prices, respectively. Garman & Klass (1980) extended the basic range estimator to include information on the open and closing prices to give,

$$V_{t,gk} = 0.5(\log(H_t) - \log(L_t))^2 - (2\log(2) - 1)(\log(C_t) - \log(O_t))^2. \quad (5)$$

Our objective will be to take the kernel estimate of volatility on a given day as a high precision estimate of the target volatility. We then test the various specifications

$$V_{t,n} = g(\log(H_t), \log(L_t), \log(H_{t-1}), \log(L_{t-1}), \dots) \quad (6)$$

We will estimate nonlinear forms for $g(Y)$ using a neural network, and also use nonlinear specification tests to see if there is additional information in residuals beyond the two high/low range volatility estimates. The neural network is a simple single hidden layer, feedforward architecture, as in

$$y = \sum_j a_j f\left(\sum_k b_{j,k} x_k + b_{j,0}\right) + a_0 \quad (7)$$

$$f(u) = \frac{1}{1 + e^{-u}}, \quad (8)$$

where $f(u)$ is the standard logistic function. We also estimate a cubic model to judge whether the complexity of the neural network is necessary for our problem. It is represented as,

$$d_t = \log(H_t) - \log(L_t) \quad (9)$$

$$V_{t,c2} = b_0 + b_1 d_t + b_2 d_t^2 + b_3 d_t^3 + b_4 d_{t-1} + b_5 d_{t-1}^2 + b_6 d_{t-1}^3. \quad (10)$$

In this paper, we focus on six stock market index: Dow Jones Industrials, FTSE 100, Nasdaq 100, Nikkei 225, Russel 2000, and *S&P* 500. The daily realized volatility series of these six indexes are from the Oxford-Man realized volatility library, as is described above. The daily high, low, open, and closing prices of each index come from Yahoo finance. The period we consider is from January 3, 2000 to March 2, 2012. Table 1 provides the summary

⁷ Beyond the original papers of Parkinson (1980), and Garman & Klass (1980), there are many applications of range based volatility estimators. Chou, Chou & Liu (2009) is a recent survey of the literature. Extensions and improvements to these early estimators are in Kunitomo (1992) and Yang & Zhang (2000). We have tested these, but found they did not change our conclusions and results. Alizadeh, Brandt & Diebold (2002) is a modern update on the older literature.

statistics of realized volatility for the six indexes.

3 Range estimates of realized volatility

In this section, we will explore the estimation accuracy and model specification of various volatility models. First, we treat the daily realized volatility series RV_t as the benchmark, and compare it with the daily series of various volatility measures during the same time period, denoted by V_t . We measure the estimation accuracy with the mean squared error and mean absolute error,

$$MSE = \frac{1}{T} \sum_{t=1}^T (RV_t - V_t)^2 \quad (11)$$

$$MAE = \frac{1}{T} \sum_{t=1}^T |RV_t - V_t|. \quad (12)$$

We use a subset of the whole sample to estimate the neural network and cubic regression that were described in section 2. First, we randomly draw a test sample with replacement from the whole sample and put it aside. The size of the test sample is 15% of the whole sample. We then estimate the neural network and cubic regression on the remaining data. Estimation of the neural network requires drawing two samples from the remaining 85% of the data. First, a training set will be used for parameter estimation as it is used to estimate the gradients over which hill climbing takes place. To avoid over fitting a second sample, the validation set, is drawn from the same pool of data with replacement. Network training continues until a minimum is reached using sample points from the validation sample. This process is repeated 1000 times to build an ensemble of neural nets. The forecast is then given by the simple average across the networks.⁸ The cubic estimates a single set of parameters using OLS over the entire estimation (nontraining) sample. Finally, volatility is estimated using both the Parkinson, and GK based volatility estimators which involves no parameter estimation. The MSE and MAE for all these volatility measures are then calculated for the whole sample and the test sample, respectively.

Tables 2 and 3 report the MSE and MAE of the four high-low based volatility measures for the six stock indexes. For each index, the first row contains the whole sample results, while the second row contains the test sample results. One may see that for almost all the

⁸ This technique is known as bagging. It was developed in Breiman (1996), and early applications using multiple networks for forecasting can be found in Perrone & Cooper (1992), LeBaron & Weigend (1998). Hillebrand & Medeiros (2010) implement this in a volatility forecasting setting.

cases, the estimation error of the neural network and cubic regression is much smaller than that of Parkinson and GK. For example, for the Dow, the test sample MSE falls from 3.01 for the Parkinson based estimator to 0.68 for the neural network, and 0.79 for the cubic. For the FTSE the MSE drops from 1.77 for Parkinson to 0.37 for the neural network, and 0.53 for the cubic. Table 3 repeats the same results using mean absolute errors. The Dow again shows a dramatic reduction with the test sample MAE going from 1.18 for the Parkinson estimate to 0.47 for the neural network, and 0.54 for the cubic. A reasonable summary across all the series is that reductions in both MSE and MAE are dramatic when moving from the traditional range based estimators to the nonlinear estimators. The relative performance of the cubic model, in most cases, is comparable with the neural network.

The intuition for the advantage of the neural network and cubic regression over Parkinson and GK is obvious. By using a richer nonlinear relationship between high-low ranges and volatility, these two volatility measures allow for more flexibility in estimation, and therefore lead the estimation closer to the target of the realized volatility. Figures 3 and 4 graphically present this intuition. To plot these two figures, we sort all the data points according to the values of high-low range, and divide the whole sample into 120 bins according to the high-low range. The difference between the highest and the lowest high-low range in each bin is the same, while the number of data points falling into each bin is varying, with fewer observations falling into the bins with the extreme high-low ranges. We take the average of each volatility measure in each bin, and plot these averages against the median value of high-low ranges in each bin in a log-log space. Figure 3 contains the plots for all six indices, while figures 4 and 5 present only the the Dow and Nikkei, and also add the Bipower adjusted volatility estimate from the volatility database in the lower panel of each figure.⁹ The scatter points represents the observed realized volatility, which implies an obviously non-linear relationship between the high-low range and volatility. The Parkinson estimate forces a linear relationship between these two variables, and similarly, the relationship approximated by the GK method is almost linear as well. In contrast, the neural network and cubic regression correctly captures the deviation from linearity between the two variables in the data. It also appears to show some better performance than the cubic in the tails where the cubic begins to diverge from the target. The nonlinear evidence does not change much when we use to the Bipower volatility estimate. This gives some initial indication that jumps are probably not the cause for our nonlinear relationship.

So far, we have provided evidence for the advantage of the neural network and cubic regression in estimating daily volatility using range information as inputs. We will now

⁹The Bipower volatility estimate attempts to remove jumps from the volatility estimate. See Barndorff-Nielsen & Shephard (2004) for details.

formally test the various model specifications. We apply the residual-based specification test proposed by Ellison & Ellison (2000). For each volatility estimation model, we calculate the model residual series ϵ_t as

$$\epsilon_t = RV_t - V_t \quad (13)$$

where RV_t is the observed realized volatility and V_t denotes the estimated model volatility. For each volatility estimate the test statistic is constructed as

$$T = \frac{\vec{\epsilon}' W \vec{\epsilon}}{\sqrt{2s(\tilde{U} W \tilde{U})}} + FSC \quad (14)$$

In equation 14, $\vec{\epsilon}$ denotes the vector of residual series ϵ_t . \tilde{U} is a diagonal matrix with the i th element being ϵ_i . W is a symmetric matrix calculated as $X'X$, where X is the model inputs. For any matrix A , function $s(\cdot)$ is define as $s(A) = \sum_{i,j} (a_{ij}^2)^{\frac{1}{2}}$, with a_{ij} being the ij th element in matrix A . FSC is calculated as

$$FSC = \frac{1 + rank(X)}{sqrt(2)s(W)}, \quad (15)$$

where X and W is defined as above. Under the null hypothesis that the model is correctly specified, the test statistic T follows a standard normal distribution.

Table 4 exhibits the specification test results for all the six indexes. For each index, the test statistics are presented in the first row, while the corresponding p-values are shown in the second row. A small p-value implies a rejection of the null hypothesis, and therefore a mis-specification of the model. One may see that for the Parkinson and GK models, the null hypothesis is rejected at the 1% significance level for all the series. The neural network and cubic models show much weaker evidence of model misspecification. The p-values are larger than 10% in about half the cases, and both specifications are rejected at the 5% level for only one series, the Nikkei. These results provide strong evidence for model misspecification for the traditional range estimators, and some supporting evidence that we cannot reject the two nonlinear specifications that we have considered.

As an initial exploration in to what might be generating our results we replicate our previous figures with returns following a simulated intraday process with and without jumps. Volatilities for the diffusion component of returns are drawn randomly for each day from a log normal distribution,

$$\sigma_t^2 \sim e^{N(\mu_V, \sigma_V^2)} \quad (16)$$

with $\mu_V = -9.5$ and $\sigma_V^2 = 1$ which are reasonable given our initial summary statistics. We

break days down into 78 sub periods which corresponds to five minute sampling over a 6.5 hour trading day. The variance of returns over the sub period is then $\sigma_t^2/78$ conditional on no jump arriving. Using results from Andersen, Benzoni & Lund (2002) we calibrate jumps as arriving Poisson with a daily arrival rate of 0.02. Jumps are assumed to be normally distributed with a standard deviation equal to the daily return standard deviation.¹⁰ Figure 6 repeats the previous plots for the case with no jumps (upper panel) and jumps (lower panel). Neither case shows the kind of richer nonlinear specification that we saw in the real data. The realized volatility levels are distributed around the Parkinson volatility estimate. Also, there is no dramatic visual impact of jumps. It is important to realize that what we expect the jump process will look like in these figures is not clear. It impacts both types of estimators, since neither of them is a jump filtered volatility estimate. These figures can only be viewed as preliminary, but they suggest that jumps are not likely to generate the kinds of connections we are seeing between high/low range information and realized volatility levels.

4 Time series forecasting

In this section we will explore the time series forecasting properties of our various volatility estimators. We are interested in comparing the nonlinear high/low range estimators with the realized volatility estimates when used to forecast future volatility.

We follow Andersen, Bollerslev, Diebold & Labys (2003) by log transforming our daily volatility estimates. Figure 2 presents the histogram of the logarithm of realized kernel for six indexes. In most cases, the empirical distribution of the logarithm of realized kernel is very close to a normal distribution, which is denoted by the solid curve. We then build time series forecasts for the logged volatility series. Figure 1 presents the time series of the realized kernel for all six indexes. The figure shows general features of persistence. In financial markets volatility exhibits extreme persistence with positive autocorrelations going out many periods.¹¹

To deal with this persistence two basic methods have been used. Andersen et al. (2003) have used a fractional filter on the data which adjusts for a true long memory process. However, some simpler multi-horizon models appear to capture the long range persistence.¹² This has been formalized in a parsimonious time series model in Corsi (2009) that uses three

¹⁰We have experimented with this parameter up to 20 standard deviations, and our results do not qualitatively change.

¹¹ See Granger & Ding (1996) for early evidence and Andersen et al. (2003) for evidence using realized volatility measures.

¹² See, for example, Ding, Granger & Engle (1993) and LeBaron (2001).

different horizon lengths to generate near long memory in the volatility time series. Let

$$RV_{j:k} = \sum_{i=j}^k RV_i, \quad (17)$$

where $RV_{j:k}$ will represent the realized volatility over a given lagged time period. The multi-horizon model can be represented as,

$$RV_t = \beta_0 + \beta_1 RV_{t-1} + \beta_2 RV_{t-5:t-1} + \beta_3 RV_{t-21:t-1} + \epsilon_t. \quad (18)$$

We follow this structure, but will replace realized volatility with our other volatility estimates in various specifications. For example, other volatility estimates can be aggregated as in,

$$V_{j:k} = \sum_{i=j}^k V_i. \quad (19)$$

We can then project realized volatility at time t on lags of V_t as in

$$RV_t = \beta_0 + \beta_1 V_{t-1} + \beta_2 V_{t-5:t-1} + \beta_3 V_{t-21:t-1}. \quad (20)$$

We log transform this equation to,

$$rv_t = \log(RV_t) = \beta_0 + \beta_1 \log(V_{t-1}) + \beta_2 \log(V_{t-5:t-1}) + \beta_3 \log(V_{t-21:t-1}). \quad (21)$$

The volatility forecast is then constructed using the estimated parameters, $\hat{\beta}_j$, from a simple OLS regression giving a forecast

$$E_t(rv_{t+1}) = \hat{\beta}_0 + \hat{\beta}_1 \log(V_t) + \hat{\beta}_2 \log(V_{t-4:t}) + \hat{\beta}_3 \log(V_{t-20:t}). \quad (22)$$

We compare all the potential volatility estimates for V_t including the obvious base case with lagged RV itself, $V_t = RV_t$. We estimate the mean squared error as,

$$MSE = \frac{1}{T} \sum_{t=1}^T (\log(RV_t) - \log(\widehat{RV}_t))^2. \quad (23)$$

We estimate both the in-sample and out-of-sample forecasting error described in equation 23. To estimate the in-sample forecasting error, we estimate equation 22 over the whole sample and compare the forecast volatility with the real data. We also estimate out of sample forecast performance using an expanding recursive window starting at $t = 500$ days,

and expanding as each new day is added to the forecast. This set of forecasts use RV_t as the forecast target, varying the right hand side variables, including lagged RV , along with our other volatility forecasts. This experiment presents a useful benchmark, but they are not a measure of what a forecaster without access to the realized volatility measures could actually use. To better simulate this situation we reestimate the previous multi-horizon forecasting models using the different high/low range volatility measures as both dependent and independent variables as in,

$$\log(V_t) = \beta_0^* + \beta_1^* \log(V_{t-1}) + \beta_2^* \log(V_{t-5:t-1}) + \beta_3^* \log(V_{t-21:t-1}). \quad (24)$$

The parameter estimates, $\hat{\beta}_j^*$, are again determined by OLS to generate forecasts \hat{V}_{t+1} . We estimate the mean squared error using these new volatility estimates, but using the RV_t volatility as the true target as in,

$$MSE^* = \frac{1}{T} \sum_{t=1}^T (\log(RV_t) - \log(\hat{V}_t))^2, \quad (25)$$

and

$$MAE^* = \frac{1}{T} \sum_{t=1}^T |\log(RV_t) - \log(\hat{V}_t)|. \quad (26)$$

Similarly, we estimate the forecasting error for both the in-sample and out-of-sample forecasting regression.

Table 5 and Table 6 summarize the in-sample and out-of-sample MSE and MSE* for the six indexes.¹³ We will concentrate here on the out of sample results in table 6, but most of these are similar when evaluated in sample. For each index, the first and fifth row contains the MSE and MSE* for the forecasting models with different volatility estimators as the predictors. For all the cases, the smallest forecasting error occurs in the first column where realized volatility itself serves as the predictor in the forecasting regression. This should be expected. We do not expect to beat the RV model in forecasting itself. It is interesting that for the MSE measure there appears to be little difference across the range based volatility estimators.

Turning to the more realistic MSE* measure gives a different picture. For several series the neural network and cubic volatility models show improvement over the Parkinson and GK models. For example, for the Dow the MSE* for Parkinson is 0.87, and the neural network and cubic models drop these to 0.37 and 0.34 respectively. Results for NASDAQ

¹³We have found similar results for MAE and MAE*

also show improvements in MSE*. It falls from 0.50 for Parkinson to 0.42 and 0.41 for the neural network and cubic respectively. For the other four series the forecast comparisons are basically a tie between the traditional and nonlinear range estimation methods.

Next we estimate the Diebold/Mariano test (Diebold & Mariano 1995), to see whether the differences between the forecasting models are significant. For any two forecasting models with the same target and different sets of predictors, we define $d\eta_t = \eta_t^1 - \eta_t^2$ as the difference between the forecasting errors in the two models at time point t , where η_t^1 and η_t^2 refer to the forecast error in the two models, respectively. With the series of $d\eta_t (t = 1, 2, \dots, T)$, we can construct the test statistic as

$$Z = \frac{\frac{1}{T} \sum_{t=1}^T d\eta_t}{\hat{\sigma}_{d\eta}} \quad (27)$$

where $\hat{\sigma}_{d\eta}$ refers to the Newey-West standard deviation of $d\eta_t$. Under the null hypothesis that the forecast accuracy of the two models is the same, the test statistic Z follows a standard normal distribution. Following this procedure we implement several pairwise comparisons of our models. In the rows labeled “versus RK” the column model is compared to the realized kernel volatility in terms of time series forecasting. The null hypothesis is that the MSE forecasts are the same for the two models. Low p-values indicate that the low MSE model is a significant improvement over the other model in the pair. Using table 6, the out of sample forecast, the row labeled versus RK reports the p-value for the forecast comparison between the range estimators and the RK volatility estimate. It shows that the gains in MSE for this model are significant against all the other estimators. Again, the comparisons of MSE* for the nonlinear models versus Parkinson and GK are most relevant. The test shows that the gains for the Dow and NASDAQ are significant. For all other series the test results are either mixed or insignificant.

Our final predictive tests follows previous studies in using a risk management inspired objective. We will use our volatility forecasts to estimate one period ahead VaR thresholds, and analyze their performance. We will use the Corsi volatility model to forecast conditional variances which will be used to estimate conditional distribution quantiles as in Andersen et al. (2003).¹⁴

Based on the forecasting regression we estimate next period’s standard deviation using,

$$\hat{V}_{t+1}^{1/2} = E_t(V_{t+1}^{1/2}) = e^{(1/2)E_tv_{t+1}+(1/8)\sigma_v^2}, \quad (28)$$

¹⁴Also, see Christoffersen (2012 forthcoming) for a survey on backtesting and reporting VaR exceptions.

which can be used to standardize the return at $t + 1$.

$$s_{t+1} = \frac{r_{t+1}}{\widehat{V}_{t+1}^{1/2}} \quad (29)$$

We further compare the returns standardized by forecast standard deviation with the certain percentiles of appropriate distributions. We report VaR exceptions, or the estimated probability of returns falling below these quantiles. Specifically, we compare the returns standardized by the standard deviation forecast with different volatility measures with the 5th percentile of three types of target distributions: a normal distribution with the mean equal to the historical mean of s_t in Equation 29 and the standard deviation equal to 1, a student t-distribution with the mean equal to the historical mean of s_t and the degree of freedom equal to 4; and the empirical distribution of s_t from the data. The last distribution is estimated by taking the full sample returns and dividing each by the standard deviation for that day given by the contemporaneous realized volatility estimator.

Table 8 reports the fraction of returns standardized by the forecast standard deviations that lie outside the 5th percentile of the target distribution, i.e. the 5% VaR.¹⁵ The distance between this 5% VaR and its theoretical value of 0.05 depends on both the choice of target distribution and the choice of volatility measures to predict the standard deviation of return. The deviation of the fraction from 0.05 is largest when the target distribution is normal. These values are reported in the first 6 rows. For most of the series and volatility models we see that the normal tails are too thin with most estimated exceptions exceeding the 5% target.

The next 6 rows repeat this test, but the normal distribution is replaced with a student-t distribution with 4 degrees of freedom. In all cases we see exceptions now much closer to the 5% target. There is some indication of improvements in the neural network and cubic estimates which we will demonstrate graphically. The last rows of table 8 calculate exceptions using the empirical distribution of standardized returns. There again appear to be advantages to the neural net and cubic estimates.

The gains from the nonlinear models appear interesting, but are difficult to see in the tables. The gains become more dramatic in figure 7 which provides a graphical comparison of the Value at Risk calculated with return standard deviation forecast by different volatility measures, with the empirical distribution standardized returns as the target distribution. In the box plots, each box represents one column of Table 7 or Table 8 with 5% VaR calculated with standard deviation forecast by one specific volatility measure across six different indexes.

¹⁵ Similar results are found for in sample volatility estimates.

The whiskers show the largest and smallest exception probabilities, and the boxes represent the next to largest, and next to smallest values. Finally, the lines are the mean of the third and fourth ranked value (the median). Visually, this shows that the performance of the neural network and cubic volatility estimates in terms of VaR exceptions is much improved over the classical range estimators, and not far from the RK estimator. While all the volatility models have a median close to the 5% target, the variability across the different series is much smaller for the nonlinear models.

5 Conclusions

In this paper we have examined the connections between realized and range based volatility estimators. We assume the realized volatility estimators, which are adjusted for micro structure noise, as our best estimate of intraday variances. We then project these on high low range information using both traditional range formulas as well as nonlinear flexible functions. We find that in daily series the nonlinear forms offer significant improvements over the traditional range estimators in terms of fitting realized volatility targets. We also explore these modified volatility estimates in terms of time series forecasting in some simple risk management related applications. We find performance which is comparable to the realized volatility measures, and often greatly improves on the other range based estimators.

Our results can therefore be viewed both as an extensive specification test, and as a forecasting test. As a specification test the results are strong and decisive. There are nonlinear specifications using daily high/low pricing information that fit daily realized volatility better than the classical estimators which are commonly used. Furthermore, we show that there is more information than what is presented in the functional forms of these volatility representations. This is an interesting result for what is driving prices at high frequencies. We show with some simple monte-carlo experiments that this is indeed the case. Looking at simulated data driven by a Brownian motion along with discrete jumps we show that it is unlikely that the simple addition of jumps could drive our results. It is still possible that micro-structure related noise is entering in a complex fashion that impacts our high/low ranges in a way that generates the nonlinear patterns we see, but this remains a topic for future study.

While we use a very general flexible functional form in the neural network in our nonlinear function fitting, our results suggest that the nonlinear patterns may not be too complicated, and may be well represented by a simple cubic model. We find a cubic model compares favorably with our neural network specification in a wide range of tests. Given its simplicity relative to the neural network, it would seem the obvious choice for researchers interested in

applying these results. In future work we may explore the use of cubic splines which could replicate the core of the cubic model's fit along with some linear discipline in the tails.

Our second task was to put these modified volatility models to the test in a risk forecasting context. Our procedure followed much of the realized volatility literature in building basic time series models in log volatility space. We built volatility forecasts with assumptions that simulated a world where the realized volatility values were not known. We are doing this to simulate the performance of the range estimators in situations where high frequency data is unavailable. After many experiments our results can be summarized in two key results. First, the nonlinear range based estimators generate performance which is remarkably close to that from estimators using actual realized volatility numbers, and high frequency data. Second, for several series we find that the nonlinear volatility series significantly improve on the two competing classical range based estimators.

This research certainly does not close the book on what we know about volatility and range based estimation. As a matter of fact, we believe we open some new puzzles, and leave a lot of work for the future. It is a little distressing that the functional form pictures were not more similar across the different series. While the patterns are all nonlinear the exact form of the mapping from realized volatility to high low ranges appears to change across the markets we study. These may be a hinderance to using these models in real world applications, or it may be helpful in determining if micro structure noise is impacting our results.¹⁶ We are also very interested in how well these models will do when we carry them across time. One useful application is to build very long range, higher quality, daily volatility models using the extensive amount of historical high/low range information that is available. This is part of our on going research.

We have shown the dramatic improvements in range based volatility estimation by using nonlinear model specifications. We believe this opens new questions about the processes driving high frequency financial prices, and provides some new tools which should be used in many applications of dynamic risk management and forecasting.

¹⁶This would assume that we can model how micro structure noise might vary with the different institutions across these markets.

References

- Alizadeh, S., Brandt, M. W. & Diebold, F. X. (2002), ‘Range-based estimation of stochastic volatility models’, *Journal of Finance* **57**, 1047–1091.
- Andersen, T. G., Benzoni, L. & Lund, J. (2002), ‘An empirical investigation of continuous-time equity return models’, *Journal of Finance* **57**(3), 1239–1284.
- Andersen, T. G., Bollerslev, T., Christoffersen, P. F. & Diebold, F. X. (forthcoming 2012), Financial risk measurement for financial risk management, *in* G. Constantinides, M. Harris & R. M. Stulz, eds, ‘Handbook of the Economics of Finance’, Elsevier.
- Andersen, T. G., Bollerslev, T. & Diebold, F. X. (2007), ‘Roughing it up: Including jump components in the measurement, modeling and forecasting of return volatility’, *Review of Economics and Statistics* **89**, 701–720.
- Andersen, T. G., Bollerslev, T., Diebold, F. X. & Labys, P. (2003), ‘Modeling and forecasting realized volatility’, *Econometrica* **96**, 579–625.
- Bandi, F. M. & Russell, J. R. (2008), ‘Microstructure noise, realized variance, and optimal sampling’, *Review of Economic Studies* **75**(2), 339–369.
- Barndorff-Nielsen, O. E., Hansen, P. R., Lunde, A. & Shephard, N. (2008), ‘Designing realized kernels to measure the ex-post variation of equity prices in the presence of noise’, *Econometrica* **76**, 1481–1536.
- Barndorff-Nielsen, O. E., Hansen, P. R., Lunde, A. & Shephard, N. (2009), ‘Realized kernels in practice: trades and quotes’, *Econometrics Journal* **12**, C1–C32.
- Barndorff-Nielsen, O. E. & Shephard, N. (2004), ‘Power and bipower variation with stochastic volatility and jumps’, *Journal of Financial Econometrics* **2**, 1–37.
- Barndorff-Nielsen, O. E. & Shephard, N. (2010), Measuring and modeling volatility, *in* R. Cont, ed., ‘Encyclopedia of Quantitative Finance’, John Wiley, pp. 1898–1901.
- Breiman, L. (1996), ‘Bagging predictors’, *Machine Learning* **24**(2), 123–140.
URL: citeseer.nj.nec.com/breiman96bagging.html
- Chou, R. Y., Chou, H. & Liu, N. (2009), Range volatility models and their applications in finance, *in* ‘Handbook of Quantitative Finance and Risk Management’, Springer-Verlag.
- Christoffersen, P. (2012 forthcoming), Backtesting, *in* R. Cont, ed., ‘Encyclopedia of Quantitative Finance’, John Wiley.

- Corsi, F. (2009), ‘A simple approximate long-memory model of realized volatility’, *Journal of Financial Econometrics* **7**(2), 174–196.
- Corsi, F., Pirino, D. & Reno, R. (2008), Volatility forecasting: The jumps do matter, Technical report, Universita di Siena.
- Diebold, F. & Mariano, R. S. (1995), ‘Comparing predictive accuracy’, *Journal of Business and Economic Statistics* **13**(3), 253–63.
- Ding, Z., Granger, C. W. & Engle, R. F. (1993), ‘A long memory property of stock market returns and a new model’, *Journal of Empirical Finance* **1**, 83–106.
- Ellison, G. & Ellison, S. F. (2000), ‘A simple framework for nonparametric specification testing’, *Journal of Econometrics* **96**, 1–23.
- Fissel, B. E. & Sun, Y. (2010), Optimal threshold selection for realized volatility forecasts in the presense of jumps, Technical report, Dept of Economics, University of California - San Diego.
- French, K. R., Schwert, G. W. & Stambaugh, R. F. (1987), ‘Expected stock returns and volatility’, *Journal of Financial Economics* **19**, 3–29.
- Garman, M. B. & Klass, M. J. (1980), ‘On the estimation of security price volatilities from historical data’, *Journal of Business* **53**, 67–78.
- Granger, C. W. J. & Ding, Z. (1996), ‘Varieties of long memory models’, *Journal of Econometrics* **73**, 61–77.
- Hansen, P. R. & Lunde, A. (2006), ‘Realized variance and market microstructure noise (with discussion)’, *Journal of Business and Economic Statistics* **24**, 127–218.
- Heber, G., Lunde, A., Shephard, N. & Sheppard, K. K. (2009), Oxford-Mann institute’s realized library, Technical Report 0.2, Oxford-Mann Institute, University of Oxford, Oxford, UK.
- Hillebrand, E. & Medeiros, M. C. (2010), ‘The benefits of bagging for forecast models of realized volatility’, *Econometric Reviews* **29**(5-6), 571–593.
- Hutchinson, J. M., Lo, A. W. & Poggio, T. (1994), ‘A nonparametric approach to pricing and hedging derivative securities via learning networks’, *Journal of Finance* **49**, 851–890.
- Kunitomo, N. (1992), ‘Improving the Parkinson method of estimating security price volatilities’, *Journal of Business* **65**, 295–302.

- LeBaron, B. (2001), ‘Stochastic volatility as a simple generator of apparent financial power laws and long memory’, *Quantitative Finance* **1**, 621–631.
- LeBaron, B. & Weigend, A. S. (1998), ‘A bootstrap evaluation of the effect of data splitting on financial time series’, *IEEE Transactions on Neural Networks* **9**(1), 213 – 220.
- McAleer, M. & Medeiros, M. C. (2008), ‘Realized volatility: A review’, *Econometric Reviews* **27**, 10–45.
- Merton, R. C. (1980), ‘On estimating the expected return on the market: An exploratory investigation’, *Journal of Financial Economics* **8**, 323–62.
- Parkinson, M. (1980), ‘The extreme value method for estimating the variance of the rate of return’, *Journal of Business* **53**, 61–65.
- Perrone, M. P. & Cooper, L. N. (1992), When networks disagree: Ensemble methods for hybrid neural networks, Technical report, Institute for Brain and Neural Systems, Brown University.
- Yang, D. & Zhang, Q. (2000), ‘Drift-independent volatility estimation based on high, low, open, and close prices’, *Journal of Business* **73**(3), 477–491.
- Zhang, L., Mykland, P. A. & Ait-Sahalia, Y. (2005), ‘A tale of two time scales: Determining integrated volatility with noisy high-frequency data’, *Journal of the American Statistical Association* **100**, 1394–1411.

Table 1: *Realized Volatility Summary*

Original Series	Mean*10 ⁴	Std*10 ⁴	Skewness	Kurtosis	ACF(1)
Dow	1.33	2.92	13.59	329.90	0.65
FTSE	1.05	1.73	6.92	81.08	0.66
NASDAQ	1.77	3.04	7.95	116.48	0.65
Nikkei	1.26	2.05	8.75	111.25	0.72
Russell 2000	1.36	2.52	9.57	164.34	0.66
SP500	1.40	2.96	13.32	331.09	0.63

Logged series	Mean	Std	Skewness	Kurtosis	ACF(1)
Dow	-9.55	0.99	0.61	3.71	0.82
FTSE	-9.76	1.06	0.25	2.88	0.86
NASDAQ	-9.28	1.07	0.40	2.85	0.87
Nikkei	-9.41	0.87	0.32	3.80	0.77
Russell 2000	-9.45	0.94	0.61	3.93	0.75
SP500	-9.51	1.03	0.49	3.42	0.82

Basic summary statistics.

Table 2: *Volatility model estimated MSE*

		Parkinson	GK	ANN	Reg
Dow	WS	4.783	6.390	1.827	1.608
	TS	3.013	4.718	0.680	0.790
FTSE	WS	2.356	1.350	0.741	0.816
	TS	1.770	1.053	0.371	0.527
NASDAQ	WS	12.701	7.302	1.914	2.387
	TS	10.650	7.336	2.490	2.778
Nikkei	WS	2.090	1.518	0.547	0.709
	TS	4.511	3.949	0.461	0.757
Russell 2000	WS	3.846	2.658	1.060	1.592
	TS	2.542	1.369	1.471	4.191
SP500	WS	3.081	1.887	1.772	2.195
	TS	2.438	0.903	2.147	3.194

Mean Squared Error of different volatility measures.

Table 3: *Volatility model estimated MAE*

		Parkinson	GK	ANN	Reg
Dow	WS	1.235	1.563	0.544	0.606
	TS	1.183	1.522	0.465	0.544
FTSE	WS	0.587	0.483	0.365	0.380
	TS	0.565	0.466	0.328	0.360
NASDAQ	WS	1.381	1.108	0.626	0.652
	TS	1.520	1.151	0.721	0.741
Nikkei	WS	0.511	0.463	0.347	0.363
	TS	0.561	0.555	0.358	0.383
Russell 2000	WS	0.795	0.590	0.489	0.527
	TS	0.741	0.541	0.482	0.571
SP500	WS	0.604	0.515	0.447	0.498
	TS	0.589	0.472	0.429	0.487

Mean Absolute Error of different volatility measures..

Table 4: *Specification tests*

	Parkinson	GK	ANN	Reg
Dow	160.284	274.310	2.823	0.873
	(0.000)	(0.000)	(0.002)	(0.191)
FTSE	39.787	23.197	1.028	1.408
	(0.000)	(0.000)	(0.152)	(0.080)
NASDAQ	53.627	75.621	0.503	1.257
	(0.000)	(0.000)	(0.307)	(0.104)
Nikkei	3.892	10.079	1.670	1.728
	(0.000)	(0.000)	(0.047)	(0.042)
Russell 2000	33.298	5.009	1.660	1.127
	(0.000)	(0.000)	(0.048)	(0.130)
SP500	2.837	16.418	1.029	1.098
	(0.002)	(0.000)	(0.152)	(0.136)

Results of specification test.

Table 5: *Volatility forecasts MSE: In sample*

		RK	Parkinson	GK	ANN	Reg(Cubic)
Dow	MSE	0.270	0.334	0.374	0.330	0.343
	versus RK		0.000***	0.000***	0.000***	0.000***
	versus P				0.134	0.011*
	versus GK				0.000***	0.000***
Dow	MSE*	0.270	0.887	1.165	0.373	0.344
	versus RK		0.000***	0.000***	0.000***	0.000***
	versus P				0.000***	0.000***
	versus GK				0.000***	0.000***
FTSE	MSE	0.240	0.281	0.286	0.275	0.289
	versus RK		0.000***	0.000***	0.000***	0.000***
	versus P				0.003***	0.003***
	versus GK				0.008***	0.298
FTSE	MSE*	0.240	0.308	0.294	0.316	0.319
	versus RK		0.000***	0.000***	0.000***	0.000***
	versus P				0.087*	0.069*
	versus GK				0.005***	0.004***
NASDAQ	MSE	0.215	0.332	0.338	0.323	0.355
	versus RK		0.000***	0.000***	0.000***	0.000***
	versus P				0.023**	0.008***
	versus GK				0.006***	0.045**
NASDAQ	MSE*	0.215	0.446	0.427	0.391	0.393
	versus RK		0.000***	0.000***	0.000***	0.000***
	versus P				0.000***	0.001***
	versus GK				0.005***	0.040**
Nikkei	MSE	0.251	0.260	0.268	0.253	0.261
	versus RK		0.018**	0.000***	0.243	0.014**
	versus P				0.008***	0.328
	versus GK				0.001***	0.083*
Nikkei	MSE*	0.251	0.346	0.382	0.296	0.292
	versus RK		0.000***	0.000***	0.000***	0.000***
	versus P				0.002***	0.000***
	versus GK				0.000***	0.000***
Russell 2000	MSE	0.277	0.332	0.317	0.321	0.344
	versus RK		0.000***	0.000***	0.000***	0.000***
	versus P				0.000***	0.000***
	versus GK				0.225	0.000***
Russell 2000	MSE*	0.277	0.347	0.325	0.341	0.354
	versus RK		0.000***	0.000***	0.000***	0.000***
	versus P				0.135	0.174
	versus GK				0.068*	0.000***
SP500	MSE	0.261	0.270	0.277	0.264	0.287
	versus RK		0.022**	0.000***	0.243	0.000***
	versus P				0.001***	0.000***
	versus GK				0.000***	0.016**
SP500	MSE*	0.261	0.312	0.378	0.321	0.299
	versus RK		0.000***	0.000***	0.000***	0.000***
	versus P				0.306	0.100*
	versus GK				0.005***	0.000***

Time series forecasting, Mean Squared Error, in sample. '***', '**', and '*' denotes significance at 1%, 5%, and 10% significance level, respectively.

Table 6: *Volatility forecasts MSE: Out of sample*

		RK	Parkinson	GK	ANN	Reg(Cubic)
Dow	MSE	0.273	0.388	0.442	0.373	0.391
	versus RK		0.000***	0.000***	0.000***	0.000***
	versus P				0.015**	0.272
	versus GK				0.000***	0.000***
Dow	MSE*	0.273	0.873	1.140	0.370	0.342
	versus RK		0.000***	0.000***	0.000***	0.000***
	versus P				0.000***	0.000***
	versus GK				0.000***	0.000***
FTSE	MSE	0.239	0.288	0.291	0.282	0.298
	versus RK		0.000***	0.000***	0.000***	0.000***
	versus P				0.004***	0.003***
	versus GK				0.051*	0.113
FTSE	MSE*	0.239	0.313	0.300	0.317	0.321
	versus RK		0.000***	0.000***	0.000***	0.000***
	versus P				0.290	0.172
	versus GK				0.039**	0.021**
NASDAQ	MSE	0.216	0.350	0.351	0.337	0.371
	versus RK		0.000***	0.000***	0.000***	0.000***
	versus P				0.012**	0.028**
	versus GK				0.018**	0.051*
NASDAQ	MSE*	0.216	0.501	0.475	0.422	0.411
	versus RK		0.000***	0.000***	0.000***	0.000***
	versus P				0.000***	0.000***
	versus GK				0.001***	0.003***
Nikkei	MSE	0.258	0.269	0.275	0.263	0.272
	versus RK		0.011**	0.002***	0.117	0.005***
	versus P				0.034**	0.189
	versus GK				0.011***	0.323
Nikkei	MSE*	0.258	0.328	0.356	0.314	0.305
	versus RK		0.000***	0.000***	0.000***	0.000***
	versus P				0.243	0.105
	versus GK				0.027**	0.006***
Russell 2000	MSE	0.269	0.354	0.331	0.339	0.365
	versus RK		0.000***	0.000***	0.000***	0.000***
	versus P				0.000***	0.001***
	versus GK				0.097*	0.000***
Russell 2000	MSE*	0.269	0.325	0.325	0.315	0.339
	versus RK		0.000***	0.000***	0.000***	0.000***
	versus P				0.032**	0.013**
	versus GK				0.199	0.067*
SP500	MSE	0.265	0.278	0.284	0.271	0.296
	versus RK		0.003***	0.000***	0.076*	0.000***
	versus P				0.000***	0.000***
	versus GK				0.000***	0.003***
SP500	MSE*	0.265	0.317	0.382	0.337	0.315
	versus RK		0.000***	0.000***	0.000***	0.000***
	versus P				0.147	0.424
	versus GK				0.037**	0.000***

Time series forecasting, Mean Squared Error, out of sample. '***', '**', and '*' denotes significance at 1%, 5%, and 10% significance level, respectively.

Table 7: *VaR: In sample*

		RK	Parkinson	GK	ANN	Reg(Cubic)
Gaussian	Dow	0.080	0.033	0.024	0.075	0.079
	FTSE	0.117	0.091	0.098	0.109	0.108
	NASDAQ	0.162	0.113	0.121	0.148	0.152
	Nikkei	0.139	0.149	0.156	0.132	0.135
	Russell 2000	0.153	0.121	0.147	0.149	0.146
	SP500	0.096	0.095	0.110	0.083	0.079
Student-t(4)	Dow	0.038	0.009	0.006	0.036	0.038
	FTSE	0.068	0.046	0.053	0.063	0.060
	NASDAQ	0.110	0.055	0.062	0.093	0.102
	Nikkei	0.085	0.094	0.098	0.075	0.082
	Russell 2000	0.095	0.055	0.079	0.085	0.079
	SP500	0.043	0.049	0.055	0.038	0.035
Empirical	Dow	0.065	0.023	0.017	0.059	0.058
	FTSE	0.069	0.048	0.053	0.064	0.061
	NASDAQ	0.049	0.013	0.015	0.037	0.046
	Nikkei	0.074	0.080	0.086	0.066	0.070
	Russell 2000	0.059	0.035	0.048	0.056	0.055
	SP500	0.062	0.064	0.077	0.056	0.048

Time series forecasting, Value-at-Risk, in sample.

Table 8: *VaR: Out of sample*

		RK	Parkinson	GK	ANN	Reg(Cubic)
Gaussian	Dow	0.069	0.029	0.022	0.067	0.070
	FTSE	0.101	0.075	0.082	0.091	0.089
	NASDAQ	0.134	0.081	0.088	0.116	0.123
	Nikkei	0.127	0.133	0.139	0.117	0.122
	Russell 2000	0.135	0.105	0.135	0.137	0.129
	SP500	0.081	0.081	0.092	0.070	0.070
Student-t(4)	Dow	0.033	0.008	0.004	0.034	0.037
	FTSE	0.058	0.036	0.042	0.049	0.050
	NASDAQ	0.078	0.033	0.039	0.066	0.074
	Nikkei	0.076	0.080	0.087	0.067	0.070
	Russell 2000	0.080	0.050	0.067	0.074	0.072
	SP500	0.039	0.042	0.048	0.035	0.035
Empirical	Dow	0.065	0.025	0.018	0.063	0.064
	FTSE	0.067	0.047	0.051	0.062	0.058
	NASDAQ	0.044	0.013	0.014	0.034	0.043
	Nikkei	0.073	0.078	0.085	0.064	0.067
	Russell 2000	0.062	0.040	0.055	0.062	0.061
	SP500	0.060	0.063	0.075	0.054	0.050

Time series forecasting, Value at Risk, out of sample.

Figure 1: *Realized volatility time series*

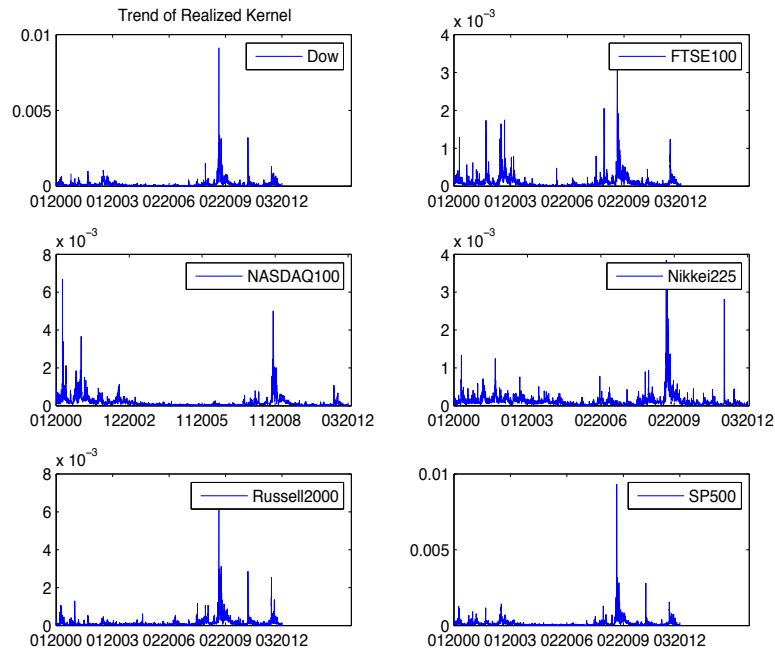


Figure 2: Log Realized volatility densities

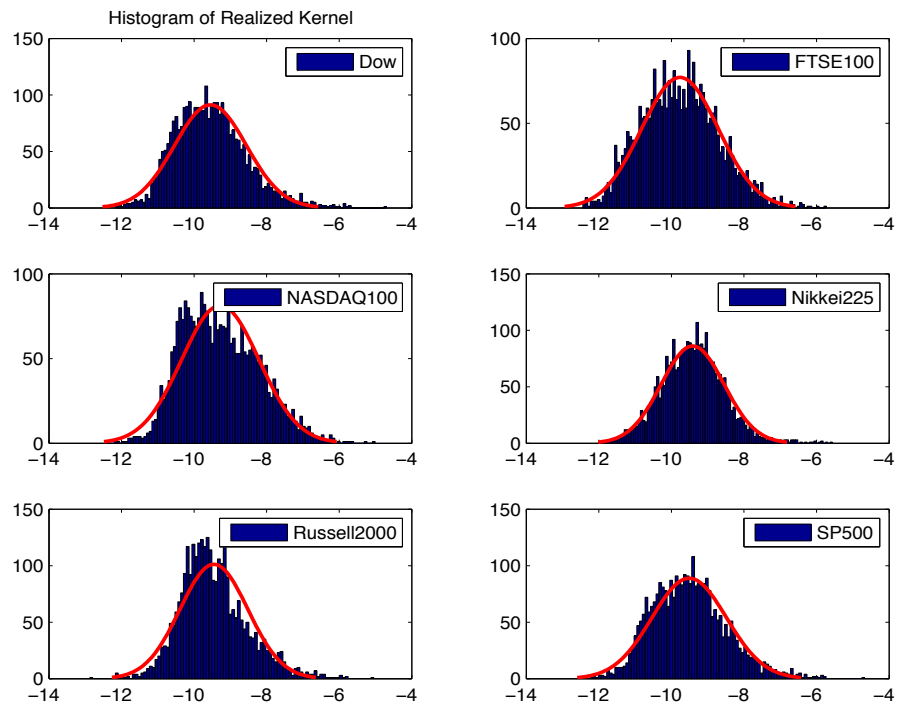
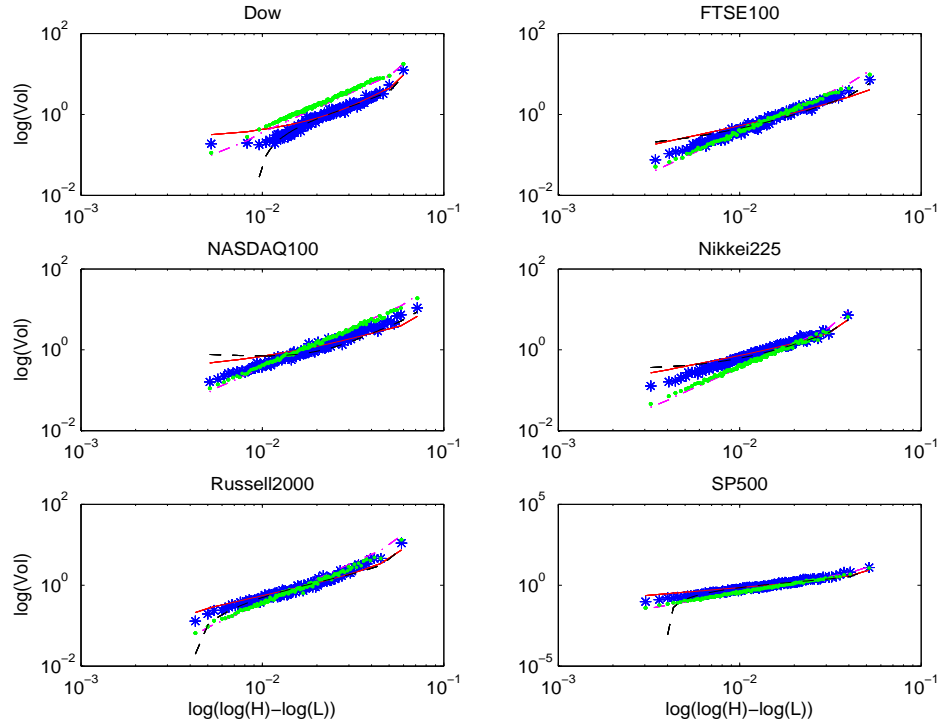


Figure 3: *Volatility and H-L ranges for all the six indexes*



'*' refers to realized volatility; the line with dash and dot represents the Parkinson volatility; the dots refer to GK volatility; the solid line represents the neural network based volatility; and the dash line represents the cubic regression based volatility.

Figure 4: *Volatility and H-L ranges for Dow*

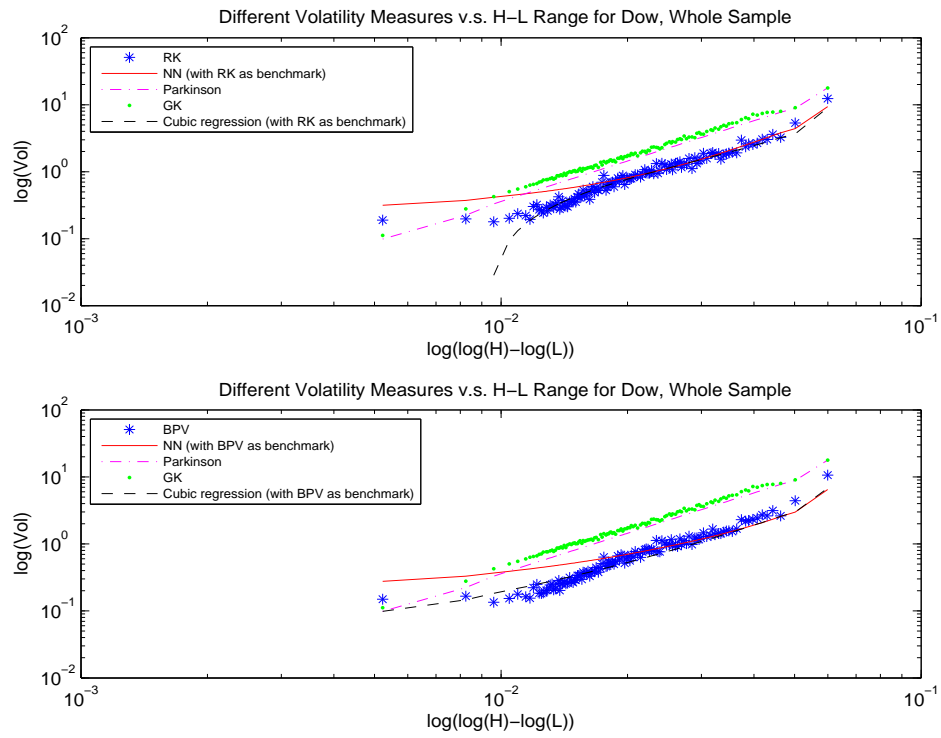


Figure 5: *Volatility and H-L ranges for Nikkei*

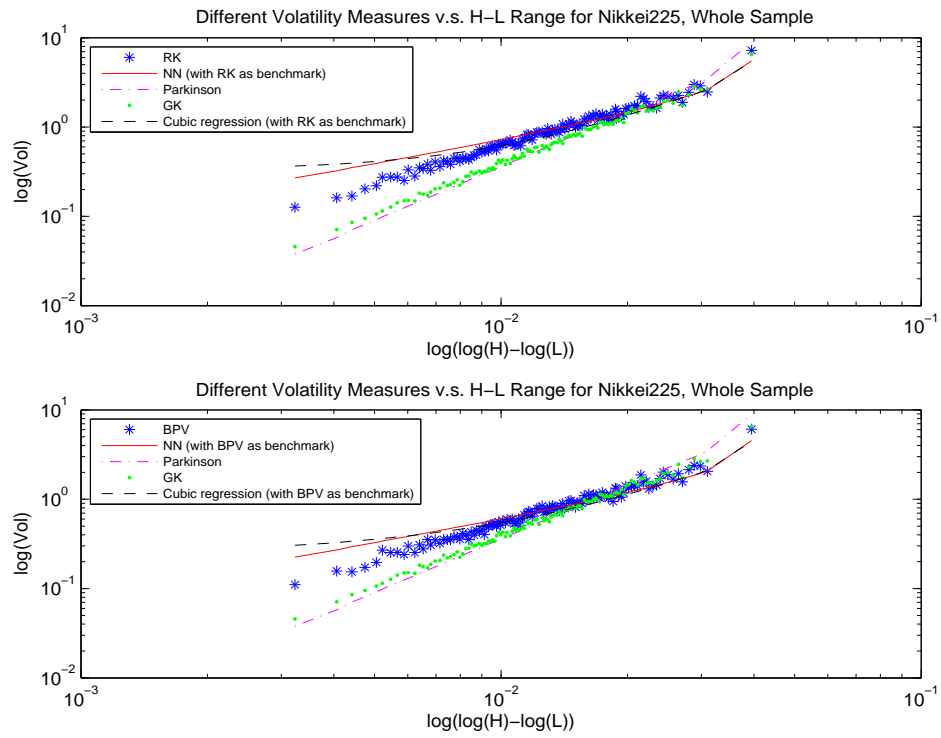


Figure 6: *Simulated jump returns*

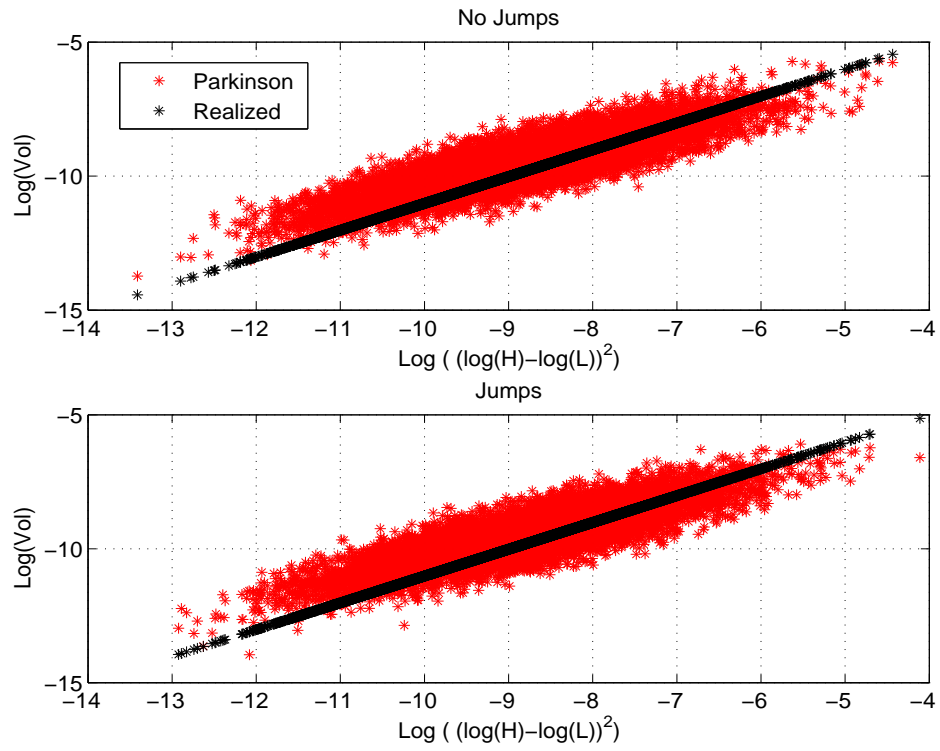
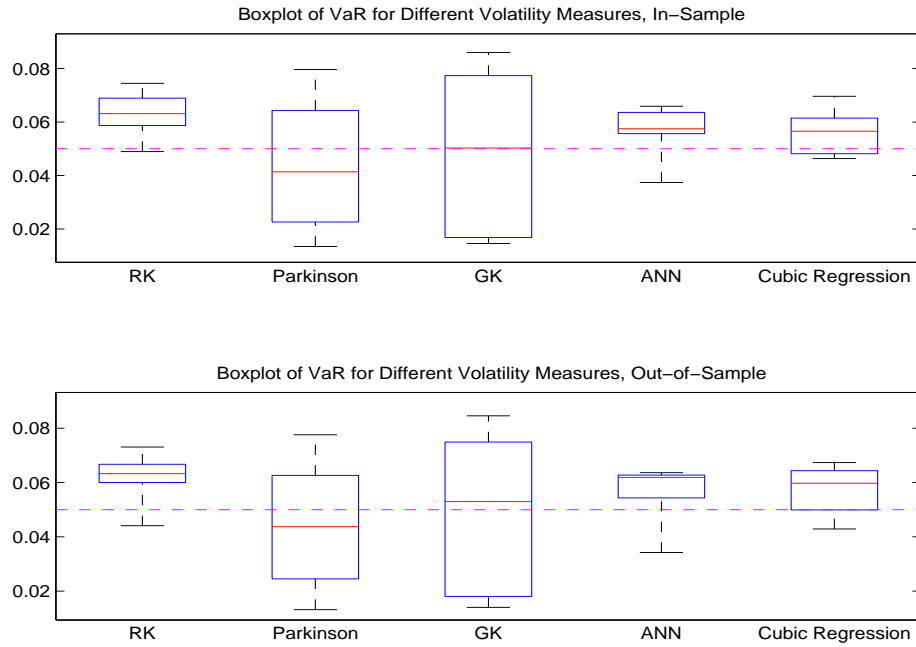


Figure 7: Box Plots of Value-at-Risk for Different Volatility Measures



The lower edge, upper edges, and the inside line of each rectangular represent the 25 percentile, 75 percentile, and median of data in each column, respectively. The whiskers below and above each rectangular refer to the minimum and maximum values of data in each column, respectively. The dash line denotes the theoretical value of 0.05.